IDENTIFICATION OF METABOLITES AND THERMAL TRANSFORMATION PRODUCTS OF QUINOLONES IN RAW COW MILK BY LIQUID CHROMATOGRAPHY COUPLED TO HIGH RESOLUTION MASS SPECTROMETRY

A. Junza[1], S. Barbosa[2], R. Codony[3], A. Jubert[3], J. Barbosa[1,2], D. Barrón[1]*

[1]Universitat de Barcelona, Departament de Química Analítica, Campus de l'Alimentació de Torribera.
Avda. Prat de la Riba, 171, 08921 Sta. Coloma de Gramanet, Barcelona, Spain

[2]Universitat de Bracelona, Departament de Química Analítica,
Martí i Franquès, 1-11, 08028 Barcelona, Spain

[3] Laboratori Interprofessional Lleter de Catalunya (ALLIC)
Ctra. Vilassar a Cabrils s/n, 08348 Cabrils, Barcelona, Spain

* To whom correspondence should be sent.
Phone: +34-934033797
E-mail: dolores.barron@ub.edu

ABSTRACT

The presence of residues of antibiotics, metabolites and thermal transformation products (TPs), produced during thermal treatment to eliminate pathogenic microorganisms in milk, could be represent a risk for people.

Cow milk samples spiked with enrofloxacin (ENR), ciprofloxacin (CIP), difloxacin (DIF) and sarafloxacin (SAR) and milk samples from cows medicated with ENR were submitted to several thermal treatments. The milk samples were analysed by liquid chromatography mass spectrometry (LC-MS) to find and identify TPs and metabolites. In this work, 27 TPs of four quinolones and 24 metabolites of ENR were found. Some of these compounds had been reported previously, but others were characterized for the first time, including lactose-conjugated CIP, the formamidation reaction for CIP and SAR, and hydroxylation or ketone formation to produce three different isomers for all quinolones studied.

Keywords: antibiotics, milk, quinolones, thermal treatments, transformation products, metabolites, elucidation, ToF, LTQ-Orbitrap

1. INTRODUCTION

Quinolones are one of the classes of antibiotics that are most widely used in veterinary practice to treat bacterial infections of animals in livestock farming and bovine milk production. Antibiotics are also used as growth promoters, although this practice has been forbidden by the European Union (EU) since 2006[1].

The presence of antibiotic residues in food is a potential risk to consumers because of direct toxic effects such as allergic reactions or the induction of resistant strains of bacteria[2,3]. To ensure human health, the EU has established maximum residue limits (MRL) for some antibiotics in foodstuffs of animal origin (37/2010/EC)[4]. Active substances are usually included in this regulation. However, their metabolites such as ciprofloxacin, the main metabolite of enrofloxacin, are only considered in a few cases.

Milk is one of the most commonly consumed foods in the world. Drug residues and metabolites can be found in milk if the time between drug administration and milking is too short. Before consumption, cow milk has to be subjected to thermal treatment to eliminate pathogenic microorganisms. Two common thermal processes are pasteurization, which consists of heating at 60ºC for 30 min or at 72ºC for 15 s, and sterilization, by which milk is heated at 120ºC for 20 min[5,6]. During thermal processes, the antibiotic residues and their metabolites could undergo transformations, depending on the temperature and the duration of the process.

The study of metabolites and their thermal degradation products is of interest because these new compounds may be a health risk to consumers and could be more persistent and harmful than the drug administered[7].

Numerous papers have been published on analytical methods to determine target substances and their main metabolites in several matrices[8-21]. However, there are few studies on the identification and determination of metabolites, degradation, and transformation products (TPs). The analytical methods consist of chromatographic separation prior to detection with a mass spectrometer. Several strategies are used to identify non-targets, including accurate mass measurement to determine the elemental composition and distinguish isobaric molecular ions, multiple mass fragmentations (MS^n), and complementary techniques such as NMR to confirm structure[7,22-34]. Some metabolites of quinolones are described in the bibliography[25,35-41], but to our knowledge no study has been carried out on metabolites in milk which has been exposed to thermal treatment.

The aim of this study was to characterize the metabolites and TPs of four quinolones ENR, CIP, DIF and SAR (Figure 1) in cow's milk subjected to thermal treatment. In order to test the new metabolites and TPs found in spiked milk samples, milk samples from animals medicated with ENR were submitted to the same thermal treatment. Samples were analysed by liquid chromatography (LC) coupled to high resolution mass spectrometry (ToF and LTQ-Orbitrap).

2. EXPERIMENTAL PROCEDURES

2.1. Chemicals and apparatus

The standards were purchased from several pharmaceutical firms: ENR from Cenavisa (Reus, Spain), CIP from Ipsen Pharma (Barcelona, Spain), DIF from Abbott (Madrid, Spain) and SAR from AK Scientific Inc. (CA,USA).

All reagents were of analytical grade unless indicated. Formic acid (HOCHO), acetic acid (HOAc), acetonitrile (MeCN), methanol (MeOH), sodium dihydrogenphosphate and sodium hydroxide (NaOH) were supplied by Merck (Darmstadt, Germany). Water was ultrapurified by a Milli-Q system (Millipore, MA, USA).

The quinolone individual stock solutions (ENR, CIP, DIF and SAR) were prepared at a concentration of 500 $\mu g \cdot mL^{-1}$ in 50 mM HOAc aqueous solution. The individual working solutions that were used to spike the milk samples were prepared by dilution of the individual stock solution at a concentration of 20 $\mu g \cdot mL^{-1}$ in water.

Sodium dihydrogenphosphate solution 0.1 M adjusted with NaOH 5 M to pH 10 was added to milk samples prior to the clean-up step.

The SPE cartridges used in this study were Oasis HLB (3 cm^3/60 mg), obtained from Waters (Milford, MA, USA).

To simulate the thermal treatment of milk, a laboratory oven (Memmert) was used to warm the samples. A Rotanta 460RS (Hettich Zentrifuguen, Germany) centrifuge was used to separate precipitated proteins and fat of supernatant after the extraction. The SPE step was carried out in a Supelco vacuum manifold with disposable liners for 24 cartridges (Bellefonte, PA, USA), connected to a Supelco vacuum tank. Evaporation to dryness was performed in a TurboVap LV (Caliper Life Science, Hopkinton, MA, USA). A Crison 2002 potentiometer (±0.1 mV) (Crison, Barcelona, Spain) with a Crison 5203 combined pH electrode from Orion Research (Boston, MA, USA) was used to measure the pH of the phosphate solution and the mobile phase.

2.2. Milk samples

Milk samples used in the work have been supplied by the Laboratori Interprofessional Lleter de Catalunya (ALLIC), control laboratory of milk in Catalonia. The samples were analysed previously in ALLIC using a screening method to determine if the milk contained residues of antibiotics. The milk samples that were negative in antibiotics were used as blank samples in this work. Four positive samples in ENR were used to study the metabolites.

2.3. LC-MS instrumentation and working conditions

2.3.1. LC conditions

Quinolones, their metabolites and degradation products were separated in a Zorbax Eclipse XDB-C8 column (5 μm, 4.6 × 150 mm) from Agilent Technologies (Santa Clara, CA, USA), using a pre-column Kromasil C8 (5 μm, 4.6 × 15 mm) supplied by Akady (Barcelona, Spain) when samples were analysed by LC-ToF. A Pursuit UPS C18 column (2.4 μm, 2 × 50 mm) from Varian (Harbor City, CA, USA) was used when samples were injected into the LC-LTQ-Orbitrap.

For both columns, the mobile phase was composed of an aqueous solution of 0.1% HOCHO (solvent A) and MeCN with 0.1% HOCHO (solvent B) at a constant flow rate of 1 $mL \cdot min^{-1}$ and 0.3 $mL \cdot min^{-1}$, respectively. The injection volume was 20 μL in LC-ToF and 10 μL in LC-LTQ-Orbitrap. Separations were carried out in a Zorbax Eclipse XDB-C8 column for 11 min under the following gradients: from 0 to 1 min, 15% B; 4 min, 45% B; 7 min, 56% B; 8.5 min, 15% B; and 11 min, 15% B. Separations were carried out in a Pursuit UPS C18 column under the following conditions: from 0 to 3.5 min, 1% B; 4.5

min, 25% B; 5 min, 50% B; 6.5 min, 50% B; 7.5 min, 25% B; 8.5 min, 10% B; and 11 min, 1% B.

2.3.2. LC-MS (ToF)

A HP Agilent Technologies 1100 LC system was equipped with an autosampler and coupled to a 6220 oa-ToF LC/MS mass spectrometer with an electrospray ionisation source (ESI) (Agilent Technologies, Santa Clara, CA, USA). The system was controlled by Mass Hunter workstation software (Agilent Technologies, Santa Clara, CA, USA) for the acquisition and processing of data from the ToF mass spectrometer.

The optimum parameters of ToF in positive mode were as follows: capillary voltage 4000 V, drying gas (N_2) temperature 300ºC, drying gas (N_2) flow rate 9 $L \cdot min^{-1}$, nebulizer gas (N_2) 40 psi, fragmentor voltage 150 V, skimmer voltage 60 V, and OCT 1 RF voltage 250 V. The ToF-MS mass resolving power was approximately 10,000 FWHM (Full width at half maximum) at *m/z* 922. Spectra were acquired over the *m/z* 50-1100 range. Data storage was in profile and centroid modes.

2.3.3. LC-MS (LTQ-Orbitrap)

An Accela LC system (Thermo Scientific, Hemel Hempstead, UK) was equipped with a thermostatic autosampler and coupled to an LTQ Orbitrap Velos mass spectrometer (Thermo Scientific, Hemel Hempstead, UK), with an ESI source. XCalibur software was used for the data analyses.

169 The operation parameters used were source voltage, 3.5 kV; sheath gas (N_2): 40 (arbitrary
170 units); auxiliary gas (N_2): 10 (arbitrary units); sweep gas (N_2): 10 (arbitrary units); and
171 capillary temperature, 275°C. Default values were used for most other acquisition
172 parameters (Fourier transform (FT) automatic gain control (AGC) target $1 \cdot 10^6$ for MS
173 mode and $5 \cdot 10^4$ for MS^n mode). Milk samples were first analysed in full MS mode with the
174 Orbitrap mass resolving power set at 30,000 FWHM at *m/z* 400. The following analyses
175 were carried out in MS^n mode with the Orbitrap mass resolving power set at 15,000
176 FWHM at *m/z* 400. The maximum injection time was set to 100 ms with one micro scan
177 for MS mode and to 500 ms with one micro scan for MS^n mode. TPs were fragmented in
178 the HCD Collision Cell because some metabolites were not fragmented in the trap. The
179 selected HCD voltage was 45 V, although in some cases it was raised to 50 and 60 V. The
180 mass range was from *m/z* 100 to 1000.
181
182 **2.4. Procedures**
183 **2.4.1 Thermal study**
184 In this study, individual standards of quinolones (ENR, CIP, DIF and SAR) at 1 $\mu g \cdot mL^{-1}$ in
185 water were warmed to degrade the antibiotics. All quinolones were heat-treated under
186 conditions of temperature and time corresponding to three thermal processes of milk:
187 pasteurization at 60ºC for 30 min (T1) or 72ºC for 15 s (T2) and sterilization at 120ºC for
188 20 min (T3). Subsequently, individual milk samples spiked with ENR, CIP, DIF and SAR
189 were warmed at 120ºC for 20 and 60 min (T3.20 and T3.60). The samples heated at
190 different temperatures were compared with spiked non-heated samples (T0) and with blank
191 milk samples at same thermal condition, ie, for example samples at T3.20 were compared
192 with blank at T3.20. Milk samples from animals medicated with ENR were also thermally

treated at T3.20 and T3.60 and compared with the same sample but non-heated. All experiments were made by triplicate.

2.4.2. Sample treatment and clean-up (SPE)

The method for analyzing the milk sample was used previously to determine the antibiotics in the milk[9-12]. The extraction method consist of the addition of 0.5 mL of phosphate solution 0.1 M at pH 10 and 2 mL of water to 2 g of milk, centrifugation of samples, and an SPE process. The SPE cartridges used were Oasis HLB and these were preconditioned with 1 mL of MeOH, 1 mL of water and 1 mL of 0.1 M phosphate solution at pH 10. After sample loading, the cartridge was washed with 3 mL of water and the analytes were eluted with 2 mL of MeOH.

The methanolic fraction eluted from the SPE was evaporated to dryness under a nitrogen stream by TurboVap LV and a water temperature of 35ºC. The extract was then reconstituted with 200 µL of water and filtered through membrane filters (Ultra free Durapore PVDF 0.22 µm from Millipore), before injection into the LC-LTQ-Orbitrap.

2.4.2. Data treatment

The LC-ToF data were treated using two procedures to find metabolites and TPs in milk samples from medicated cow with ENR. The first corresponds to the manual comparison of mass spectra of blanks and samples. This procedure was used initially to detect the TPs in standards and spiked cow milk. The other option consists of the use of Mzmine2[42,43] free software, which provides a list of all *m/z* on mass spectra. The list can be shortened by removing all the ions that only appear in the blank spectra and those that have a similar or higher intensity in the blanks than in the samples. Only the ions which appeared between 1

to 9 min and from 150 to 800 Da were considered. Also, a mass defect filter (MDF) of 120 mDa was applied.

3. RESULTS AND DISCUSSION

3.1. Determination of thermal TPs by LC-ToF-MS

Blank and spiked water samples were subjected to the thermal conditions explained in Section 2.3.1 and analysed by LC-ToF-MS. The total ion current chromatograms (TIC) of spiked water samples were compared with the TIC of blank water samples to examine for possible TPs. The two chromatograms were nearly identical, except for the spiked antibiotic peak.

The mass spectra of blank and spiked water samples were compared by overlapping. The only difference between the spiked sample and the blanks was the peak of parent compound. However, a decrease in the area of the protonated molecule of quinolones was noticed when the temperature rose. The highest decrease was seen when the samples were heated at 120ºC for 20 min (T3.20) where in some cases up to 20%. A new condition of 120ºC for 60 min (T3.60) was also applied to ensure that TPs were obtained in sufficient high concentrations to be detected.

Raw cow milk samples free of quinolones were spiked and heated under the selected conditions. To assess whether any TPs had formed, the same procedure as that used for the water standards was followed. In this case, some ions were identified in the mass spectra of the spiked milk samples that were not observed in the blank milk samples. Some ions were identified as doubly charged protonated molecules, with characteristic losses of water and

carbon dioxide. These ions were also detected in the water samples. The doubly protonated identity was confirmed by the isotopic pattern. The difference between $[M+2H]^{2+}$ and $[M+1+2H]^{2+}$ was *m/z* 0.5. In addition, the same retention time (t_R) of the compounds in the extracted ion chromatogram (EIC) was observed[44]. The losses of H_2O (18.0105) and CO_2 (43.9898) are not considered as TPs because these were also observed in the source by CID-in-source fragmentation[40,45-48]. The ions *m/z* 332.1405 and 386.1311 were detected in samples that were spiked with ENR and DIF respectively. These *m/z* values are consistent with the *m/z* of CIP and SAR. The EIC were obtained for blank and spiked samples to check the presence of TPs. Table 1 shows all the ions found in milk and their identification, sorted by the original antibiotic. As can be observed, the errors between experimental mass and assigned structure were lower than 3.0 ppm.

To assign a structure to the remaining of the ions that were observed, an in-house database was created using a list of 106 metabolic reactions[49] that can take place in milk, and another list of milk components (including carbohydrates, amino acids, vitamins and lipids; a total of 188 components)[50]. The exact mass of the starting antibiotic or a known fragment is introduced into the database and a series of combinations of reactions and/or possible additions are obtained that give rise to a molecule with an exact mass similar to that observed in the mass spectra of ToF.

3.2. Identification of thermal TPs by LC-LTQ-Orbitrap-MS

As a ToF spectrometer cannot fragment molecules, we used an LTQ-Orbitrap to elucidate the TPs, as it has a higher mass resolving power than ToF and can fragment the compound to obtain structural information.

For each quinolone, Table 2 shows the retention time (t_R), *m/z* values, the gains and losses of mass compared to the parent quinolone, the *m/z* of the TPs observed, and the fragments observed in mass spectra. Table 2 also shows the proposed reactions, with the assigned molecular formula, the double bond equivalents (DBE) of neutral molecules, the theoretical mass, and the error in ppm calculated for the formula. The information is provided as common reactions that occurred in all the studied quinolones, and other reactions that were only observed in some quinolones.

Common reactions of the four quinolones

Several gains and losses of mass were common among the four quinolones studied. Our database shows that the gain of 15.9949 *m/z* (Table 2) could correspond to two different reactions: hydroxylation and N-oxide formation. An evaluation of MS/MS spectra could be used to differentiate between both structures. As an example, Figure 2A shows the MS/MS spectrum of ions *m/z* 416.1416 in samples of DIF and discussion about elucidation is given in supporting information. The position of OH could not be assigned with certainty, but our proposal is hydroxylation in position 3 of the piperazine ring, as in oxo-ciprofloxacin, the metabolite described in the bibliography[36,37,40]. For the four quinolones, the hydroxylated-TPs were observed, but the concentration of TPs from ENR and DIF were higher than CIP and SAR ones. N-oxide formation only occurred in ENR and DIF in N^4-alkylpiperazinyl. This metabolite has been described previously[38,51]. For this structure, a loss of OH is characteristic in fragmentation and was experimentally observed in Figure 2B of the MS/MS spectrum of ions *m/z* 416.1416 for DIF. In this case, the DBEs of TPs undergo no alteration of values in comparison to the DBE of parent quinolones. Different

fragmentation patterns were observed for the hydroxylated and N-oxide compounds that were found, as can be observed in Figure 2A and B. In Figure 2B, corresponding to the N-oxide TP, the peak of the precursor ion disappeared almost completely when the same voltage was applied (HCD: 45). This finding suggests that hydroxylated compounds are more stable than N-Oxide TP. The structures assigned to the rest of the ions are shown in Figure 2. Table 2 shows the fragmentation ions, the molecular formula, the DBE, and the calculated error in the assignation of the different structures.

A gain of 29.9740 *m/z* was also observed for the four quinolones, as shown in Table 2. Three peaks were found for ENR and DIF, whereas only one peak was observed for their main metabolites (CIP and SAR), at a concentration too low to be isolated and fragmented. The mass spectra of all peaks of ENR and DIF were studied. Figure 3 shows the mass spectra of ions with *m/z* 390.1460 of ENR. In Figure 3A, the separation by LC-LTQ-Orbitrap is shown with peaks at 5.71, 7.57 and 7.99 min. Although the retention time of ENR matches peak 1, the mass spectra are different, as can be observed in Figures 3B and C. A comparison of both mass spectra revealed only two ions (m/z 245.1077 and 72.0805) in common. The *m/z* 245.1077 indicates that the differences between the TP of peak 1 and ENR are in the loss fragment (part of the piperazinyl ring). The accurate mass of the fragment *m/z* 128.0706 corresponds to molecular formula $C_6H_{10}NO_2$ with a DBE value of 3 and is the key to the elucidation as is shown in Figure 3C and in the supporting information[52].

Unlike the first molecule, the other two ions of *m/z* 390.1460 (peaks 2 and 3) had low fragmentation as can be observed in Figure 3. Nevertheless, their structures were elucidated. The retention time of these peaks are different, but their mass spectra are

identical, which indicates that they are isomers (Figure 3D). The *m/z* 245.1085 observed in the mass spectrum of ENR (Figure 3B) could not be found in the spectra of peaks 2 and 3. The molecules were broken up from the piperazinyl ring, resulting in the ions 100.0756 and 291.0774. The fragment 100.0756 is the same as that observed in Figure 3C, which indicates that there was only a ketone in the ring. The fragmentation of 291.0774 makes us to conclude that OH is on the aromatic ring. Two different vacant positions in the aromatic ring led to the two different isomers. For DIF, the fragmentations were similar to those shown in ENR, as can be observed in Table 2.

TPs corresponding to net loss of 26.0146 were observed for all compounds (ENR, CIP, DIF and SAR). For the TPs of ENR and DIF the losses of N^4-alkylamine from piperazinyl ring were observed. However, as CIP and SAR do not have an alkyl group in N^4, the losses of ammonia (17.0275) were seen. Moreover, the TPs had DBE one unit lower than the parent compound, due to the break in the piperazinyl ring. Therefore, the peaks at *m/z* 334.1560, 306.1246, 374.1307 and 360.1156 have been assigned to desethylenequinolone TPs[34-37]. As Table 2 shows, when Orbitrap was used to elucidate the structures, the calculation errors (ppm) were lower than 2 ppm. Slightly higher error values were obtained when ToF was used.

Other reactions

The major metabolites, CIP and SAR, underwent other transformations, as can be observed in Table 2. Due to the absence of the alkyl chain in the N^4-piperazinyl ring, two reactions acetylation (Acetyl-CIP (*m/z* 374.1509) and Acetyl-SAR (*m/z* 428.1416)) and formamidation (Formamide-CIP (*m/z* 375.1463) and Formamide-SAR (*m/z* 429.1416)) took place. The corresponding explanation of elucidation is in supplementary material.

In addition to the above-mentioned reactions, CIP gave three more TPs (*m/z*: 274.0986, 573.1429 and 656.2457). The ion 573.1429 was observed at a very low concentration and could not be fragmented. For the mass 274.0986, the ion 292.1091 could also be observed, at less intensity, corresponding to the gain of a water molecule. The main ion obtained by MS^2 of the ion 274.0986 was 231.0564, and this was isolated and fragmented again. In the MS^3 spectrum, the ion *m/z* 249.0668 was also observed with *m/z* 231.0564 which corresponds to gain of a water molecule. This gain of water was only observed in the ions that kept the carbonyl group of acid, which is capable of hydrating the initial carboxylic acid again. The rest of the ions were mainly due to fragmentation of the piperazine ring. The structure assigned to *m/z* 292.1091 was CIP, with loss of the cyclopropyl group.

The last TP (656.2457) was obtained by heating the spiked milk sample with CIP at T3.60. When a HCD voltage of 45 V was used, only fragments with low *m/z* were found. To obtain structural information, the voltage was reduced to 35 V. The CIP ion (*m/z* 332.1400) could be identified among all the fragments as can be seen in Figure 4. As can be followed in supporting information, the molecule CIP (332.1405) is combined with the lactose (galactose + glucose) present in milk at high concentration. This new product was favoured when samples were heated at a high temperature for a long time (60 min).

3.3. Effect of temperature on the stability of TPs

For each TP ion, the areas obtained from milk samples were plotted *vs.* the heating conditions (T0, T3.20 and T3.60) (Figure 5). For ENR and CIP (Figure 5A and 5B), all the TPs were observed at T0 except for hydroxylated quinolones (*m/z* 376.1656_1 and 348.1334, respectively). The concentration of these ions was raised by heating at T3.20, and disappeared at T3.60. In the case of ENR (Figure 5A), the concentration of some TPs,

including CIP (332.1402), desethylene-ENR (334.1569) and two isomers of hydroxylation and ketone formation (390.1461_1 and 390.1461_3), increased slightly by warming at T3.20, and decreased at T3.60. For CIP, T3.60 was required for conjugation with lactose (656.2477) to occur (Figure 5B). The acetylated (374.1535) and formamidated (375.1463) were present at T0 and their concentrations increased by heating. The 362.1148 ion (corresponding to gain $[M+H+29.974]^+$) was initially present (T0), but was destroyed by heating.

In contrast, the concentration of most of the ions in DIF samples increased slightly when the temperature was increased (Figure 5C). A general downward trend of DIF ions was seen at T3.60. Completely different behaviour was observed for the 430.1185_3 ion, which underwent sharp decrease at T3.20 and a sharp rise in formation when the warming time was increased, possibly due to the ion coming from different sources, and for the 430.1185_1 ion, which disappeared completely at T3.20. The acetylated (428.1407) and formamidated (429.1391) TPs of SAR (Figure 5D) behaved in the same way as those of CIP, *i.e.*, their concentration increased with temperature.

3.4 Determination of metabolites and TPs in medicated cow milk

Four raw milk samples from cows medicated with ENR were submitted to the same thermal treatments as the spiked milk samples. The extracts were analysed by LC-ToF and the metabolites and TPs were fragmented by LC-LTQ-Orbitrap.

In this case, metabolites and TPs were found using the two data treatments (Section 2.3.3). When exact mass, retention time and MS/MS spectra were compared, some of the compounds in milk spiked with ENR and CIP were also present in medicated cow milk.

Table 3 shows the retention time (t_R) of metabolites in samples analysed by LC-ToF, the accurate *m/z* of metabolites determined by ToF and LTQ-Orbitrap, the assigned molecular formula, the theoretical mass, the error in ppm calculated for the assigned formula, the proposed structures, and the double bond equivalents (DBE) of the neutral molecule.

CIP (*m/z* 332.1405), the main metabolite of ENR, was one of the common compounds. In addition, desethylene metabolites of ENR (*m/z* 334.1561)(ENR-6) and CIP (*m/z* 306.1248)(ENR-3) were observed. The TPs of ENR corresponded to hydroxylation (ENR-16) and N-Oxide formation (ENR-17)(*m/z* 376.1667) and two isomers of compound *m/z* 390.1460 (ENR-18 and ENR-19) (hydroxylation and ketone formation, Figure 3D) were also found. Four TPs of CIP were observed in medicated cow milk. At 3.6 min was found the hydroxy-CIP (*m/z* 348.1354)(ENR-8) and at 6.1 min the *m/z* 362.1147(ENR-11), although this time the MS^2 spectrum could not be obtained due to its low concentration. The other metabolites were from acetylation (*m/z* 374.1511)(ENR-14) and formamidation (*m/z* 375.1463)(ENR-15) of CIP.

Other compounds were found in milk from medicated cows, but not in spiked milk. These compounds were produced by metabolism of the antibiotic in the cow, and some of them were identified for the first time.

The metabolite with the highest intensity after CIP (332.1405) and desethylene-ENR (334.1561)(ENR-6) had *m/z* 263.0834 (ENR-1). The *m/z* of the metabolite was lower than the *m/z* of ENR. Therefore, the MS/MS spectrum was analysed to find which part of the parent compound had been modified. Figure 6A shows MS/MS spectrum of ENR-1. It

419 was concluded that the metabolite structure corresponded to CIP without a piperazine ring
420 (Supporting information). Only the amino group was maintained, as shown in Table 3.
421
422 In the MS/MS spectrum of metabolite ENR-2 with *m/z* 291.0783 (Figure 6B), the ion *m/z*
423 263.0834 (ENR-1), discussed above in supporting information and in Figure 6A, was
424 observed. The difference between both ions corresponded to a carbonyl group (27.9949).
425 The assigned structure for this metabolite is given in Table 3.
426
427 Another metabolite elucidated was *m/z* 307.1095 (ENR-4). Some explanations of the
428 fragments are shown in Figure 6C and supporting information. Its structure can be
429 observed in Table 3.
430
431 The ion *m/z* 334.1189 (ENR-5) was identified as formyldesethylene-CIP[25]. Its structure
432 was checked by its mass spectrum. The molecule was broken up from the piperazinyl ring,
433 resulting in the ions *m/z* 72.0445 and 263.0834 cited before. Other important fragments
434 were *m/z* 245.0730 [263.0834-H_2O], 230.0489 [334.1189-H_2O-Cyclopropyl-Formamide]
435 and 217.0411 [230.0489-CH].
436
437 A compound (ENR-9) with the same *m/z* as hydroxy-CIP (*m/z* 348.1354)(ENR-8) was also
438 studied, because the retention time differed by about 4 minutes from the peak observed in
439 spiked samples. The MS/MS spectrum (Figure 6D) was very similar to the spectrum of
440 formyldesethylene-CIP (*m/z* 334.1189)(ENR-5). The most striking difference between both
441 spectra was that instead of fragment *m/z* 72.0444 was observed a fragment of *m/z* 86.0601.
442 This fragment corresponds to the addition of a methyl group to fragment *m/z* 72.0444. In

conclusion, a structure of acetyldesethylene-CIP (ENR-9) is suggested, which could be formed from the oxidation of the side chain of desethylene-ENR (*m/z* 334.1561)(ENR-6).

The EIC of ion *m/z* 362.1137 (ENR-12 and ENR-13) from a full-scan of ToF was very similar to that obtained for the *m/z* 390.1460 (ENR-18 and ENR-19) in spiked samples with ENR (Figure 3). Three peaks were observed in the EIC. The first one was at 6.1 min, which coincides with the peak observed in samples fortified with CIP. Also were seen two peaks at 6.8 and 7.1 min, with the same shape as the two peaks at 7.6 and 7.99 in Figure 3. Unfortunately, when the sample was analysed by LC-LTQ-Orbitrap, it was degraded and only one peak was observed and fragmented. In the MS/MS spectrum, the ions *m/z* 291.0776 and 259.0820 were present, as elucidated previously in Figure 3D. Another fragment that helped to determine the structure corresponded to *m/z* 72.0444, which is like fragment 100.0757 of metabolite 390.1460 without the alkyl chain of ENR. Due to the resemblances between the EICs and mass spectra of ions *m/z* 362.1137 (ENR-12 and ENR-13) and 390.1460 (ENR-18 and ENR-19), can be assume that these compounds are the same, but one is from CIP and the other from ENR, respectively.

The last two elucidated metabolites corresponded to oxo-CIP (*m/z* 346.1198)(ENR-7) and formyl-CIP (360.1354)(ENR-10), which have been described previously in literature[36,40]. Their structures were confirmed by their MS/MS spectra.

The rest of the metabolites found in medicated cow milk could not be elucidated. In any case, Table 3 shows their *m/z*, retention time (t_R), hypothetical molecular formula, double bond equivalents (DBE) and errors in ppm.

AUTHOR INFORMATION

Funding source

The authors are grateful to the Ministerio de Ciencia e Innovación (MICINN) (Project CTQ2010-19044/BQU) for financial support. A.J. received support from MICINN (BES-2011-045849) for the training of researchers.

Supporting Information Available

Explanation about MS elucidation of some TPs and metabolites of quinolones (ENR, CIP, DIF and SAR) has been included. This material is available, free of charge, via the Internet at http://pubs.acs.org.

REFERENCES

1. Council Regulation No 1831/2003 of the European Parliament and of the Council of 22 September 2003 on additives for use in animal nutrition.

2. Hammerum, A.M.: Heuer, O.E.; Lester, C.H.; Agers, Y.; Seyfarth, A.M.; Emborg, H.D.; Frimodt-Moller, N.; Monnet, D.L. Comment on: withdrawal of growth-promoting antibiotics in Europe and its effects in relation to human health. *Int J Antimicr Agents* **2007**, 30, 466-468.

3. Fábrega, A.; Sánchez-Céspedes, J.; Soto, S.; Vila, J. Quinolone resistance in the food chain. *Int J Antimicr Agents* **2008,** 31, 307-315.

4. Commission of the European Communities, Official Journal of the European Communities No. 37/2010 L15/1, December 22, 2009.

5. Zorraquino, M.A.; Althaus, R.L.; Roca, M.; Molina, M.P. Effect oh heat treatments on aminoglycosides in milk. *J Food Prot*. **2009**, 72, 1338-1341.

6. Early, R. The technology of dairy products. Edition 2.; Ed. Aspen Publishers Inc.; Gaithersburg, Maryland, USA, **1998**.

7. Picó, Y.; Barceló, D. The expanding role of LC/MS in analyzing metabolites and degradation products of food contaminants. *Trends Anal Chem*. **2008,** 27, 821-835.

8. Becker, M.; Zittlan, E.; Petz, M. Residue analysis of 15 penicillins and cephalosporins in bovine muscle, kidney and milk by liquid chromatography–tandem mass spectrometry. *Anal Chim Acta* **2004**, 520, 19-32.

9. Junza, A.; Amatya, R.; Barrón, D.; Barbosa, J. Comparative study of the LC–MS/MS and UPLC–MS/MS for the multi-residue analysis of quinolones, penicillins and

504 cephalosporins in cow milk, and validation according to the regulation 2002/657/EC. *J*
505 *Chromatogr B* **2011,** 879, 2601-2610.
506 10. Reyns, T.; Cherlet, M.; De Baere, S.; De Backer, P.; Croubels, S. Rapid method for the
507 quantification of amoxicillin and its major metabolites in pig tissues by liquid
508 chromatography-tandem mass spectrometry with emphasis on stability issues. *J*
509 *Chromatogr B* **2008**, 861, 108-116.
510 11. Granelli, K.; Elgerud, C.; Lundström, A.; Ohlsson, A.; Sjöberg, P. Rapid multi-residue
511 analysis of antibiotics in muscle by liquid chromatography–tandem mass spectrometry.
512 *Anal Chim Acta* **2009**, 637, 87-91.
513 12. Martínez-Huélamo, M.; Jiménez-Gámez, E.; Hermo, M.P.; Barrón, D.; Barbosa, J.
514 Determination of penicillins in milk using LC-UV, LC-MS and LC-MS/MS. *J Chromatogr*
515 *A* **2009,** 32, 2385-2393.
516 13. Nemutlu, E.; Kir, S.; Katlan, D.; Beksaç, M.S. Simultaneous multiresponse
517 optimization of an HPLC method to separate seven cephalosporins in plasma and amniotic
518 fluid: Application to validation and quantification of cefepime, cefixime and cefoperazone.
519 *Talanta* **2009**, 80, 117-126.
520 14. Mol, H.G.J.; Plaza-Bolaños, P.; Zomer, P.; de Rijk, T.C.; Stolker, A.A.M.; Mulder,
521 P.P.J. Toward a Generic Extraction Method for Simultaneous Determination of Pesticides,
522 Mycotoxins, Plant Toxins, and Veterinary Drugs in Feed and Food Matrixes. *Anal Chem.*
523 **2008**, 80, 9450-9459.
524 15. Marazuela, M.D.; Bogialli, S. A review of novel strategies of sample preparation for
525 the determination of antibacterial residues in foodstuffs using liquid chromatography-based
526 analytical methods. *Anal Chim Acta* **2009**, 645, 5-17.

16. Moreno-Bondi, M. C.; Marazuela, M.D.; Herranz, S.; Rodríguez, E. An overview of sample preparation procedures for LC-MS multiclass antibiotic determination in environmental and food samples. *Anal Bioanal Chem*. **2009**,395, 921-946.

17. Blasco, C.; Torres, C.M.; Picó, Y. Progress in analysis of residual antibacterials in food. *Trends Anal Chem*. **2007**, 26, 895-913.

18. Andreu, V.; Blasco, C.; Picó, Y. Analytical strategies to determine quinolone residues in food and the environment. *Trends Anal Chem***. 2007,** 26, 534-556.

19. Bogialli, S.; Di Corcia, A. Recent applications of liquid chromatography–mass spectrometry to residue analysis of antimicrobials in food of animal origin. *Anal Bioanal Chem*. **2009**, 395, 947-966.

20. Tang, Q.; Yang, T.; Tan, X.; Luo, J. Simultaneous Determination of Fluoroquinolone Antibiotic Residues in Milk Sample by Solid-Phase Extraction - Liquid Chromatography - Tandem Mass Spectrometry. *J.Agric. Food Chem*. **2009**, 57, 4535-4539.

21. Romero-González, R.; Aguilera-Luiz, M.M.; Plaza-Bolaños, P.; Garrido Frenich, A.; Martínez Vidal, J.L. Food contaminant analysis at high resolution mass spectrometry: Application for the determination of veterinary drugs in milk. *J Chromatogr A* **2011**, 1218, 9353-9365.

22. Kaufmann, A. Strategy for the elucidation of elemental compositions of trace analytes based on a mass resolution of 100 000 full width at half maximum. *Rapid Commun Mass Spectrom*. **2010,** 24, 2035-2045.

23. Zhu, M.; Ma, L.; Zhang, D.; Ray, K.; Zhao, W.; Humphreys, W.G.; Skiles, G.; Sanders, M.; Zhang, H. Detection and Characterization of Metabolites in Biological Matrices Using Mass Defect Filtering of Liquid Chromatography/High Resolution Mass Spectrometry Data. *Drug Metab Dispos* **2006**, 34, 1722-1733.

551 24. Nägele, E.; Moritz, R. Structure Elucidation of Degradation Products of the Antibiotic
552 Amoxicillin with Ion Trap MSn and Accurate Mass Determination by ESI TOF. *J Am Soc*
553 *Mass Spectr*. **2005**, 16, 1670-1676.
554 25. Calza, P.; Medana, C.; Carbone, F.; Giancotti, V.; Baiocchi, C. Characterization of
555 intermediate compounds formed upon photoinduced degradation of quinolones by high-
556 performance liquid chromatography/high-resolution multiple-stage mass spectrometry.
557 *Rapid Commun Mass Spectrom*. **2008**, 22, 1533-1552.
558 26. Gómez, M.J; Gómez-Ramos, M.M.; Malato, O.; Mezcua, M.; Fernández-Alba, A.R.
559 Rapid automated screening, identification and quantification of organic micro-
560 contaminants and their main transformation products in wastewater and river waters using
561 liquid chromatography–quadrupole-time-of-flight mass spectrometry with an accurate-
562 mass database. *J Chromatogr A* **2010,** 1217, 7038-7054.
563 27. Kaufmann, A. Determination of the elemental composition of trace analytes in complex
564 matrices using exact masses of product ions and corresponding neutral losses. *Rapid*
565 *Commun Mass Spectrom*. **2007,** 21, 2003-2013.
566 28. Berendsen, B.J.A.; Essers, M.L.: Mulder, P.P.J.; van Bruchem Lommen, A.; van
567 Overbeek, W.M., Stolker, L.A.M. Newly identified degradation products of ceftiofur and
568 cephapirin impact the analytical approach for quantitative analysis of kidney. *J*
569 *Chromatogr A* **2009**, 1216, 8177-8186.
570 29. Krauss, M.; Singer, H.; Hollonder, J. LC–high resolution MS in environmental
571 analysis: from target screening to the identification of unknowns. *Anal Bioanal Chem*.
572 **2010**, 397, 943-951.
573 30. Prasad, B.; Garg, A.; Takwani, H.; Singh, S. Metabolite identification by liquid
574 chromatography-mass spectrometry. *Trends Anal Chem*. **2011,** 30, 360-387.

575 31. Lacorte, S.; Fernández-Alba, A.R. Time of flight mass spectrometry applied to the
576 liquid chromatography analysis of pesticides in water and food. *Mass Spectrom Rev*. **2006,**
577 25, 866-880.
578 32. Malik, A.K.; Blasco, C.; Picó, Y. Liquid chromatography–mass spectrometry in food
579 safety. *J Chromatogr A* **2010,** 1217, 4018-4040.
580 33. Koulman, A.; Lane, G.A.; Harrison, S.J.; Volmer, D.A. From differentiating
581 metabolites to biomarkers. *Anal Bioanal Chem*. **2009,** 394, 663-670.
582 34. Jacobs, D.M.; Spiesser, L.; Garnier, M.; de Roo, N.; van Dorsten Hollebrands, B.; van
583 Velzen, E.; Draijer, R.; van Duynhoven, J. SPE–NMR metabolite sub-profiling of urine.
584 *Anal Bioanal Chem*. **2012,** 404, 2349-2361.
585 35. Sturini, M.; Speltini, A.; Maraschi, F.; Profumo, A.; Pretali, L.; Fasani, E.; Albini, A.
586 Photochemical Degradation of Marbofloxacin and Enrofloxacin in Natural Waters. *Envir*
587 *Sci Thecno*. **2010,** l44, 4564-4569.
588 36. Anadón, A.; Martínez-Larrañaga, M.R.; Iturbe, J.; Martínez, M.A.; Díaz, M.J.; Frejo,
589 M.T.; Martínez, M. Pharmacokinetics and residues of ciprofloxacin and its metabolites in
590 broiler chickens. *Res Vet Sci*. **2001,** 71, 101-109.
591 37. Turnipseed, S. B.; Storey, J.M.; Clark, S.B.; Miller, K.E. Analysis of Veterinary Drugs
592 and Metabolites in Milk Using Quadrupole Time-of-Flight Liquid Chromatography−Mass
593 Spectrometry. *J Agric Food Chem*. **2011,** 59, 7569-7581.
594 38. Sukul, P.; Lamshöft, M.; Kusari, S.; Zühlke, S.; Spiteller, M. Metabolism and excretion
595 kinetics of 14C-labeled and non-labeled difloxacin in pigs after oral administration, and
596 antimicrobial activity of manure containing difloxacin and its metabolites. *Environ Res.*
597 **2009,** 109, 225-231.

598 39. Turiel, E.; Bordin, G.; Rodríguez, A.R. Study of the evolution and degradation
599 products of ciprofloxacin and oxolinic acid in river water samples by HPLC-UV/MS/MS-
600 MS. *J Environ Monit*. **2005,** 7, 189-195.
601 40. Volmer, D.A.; Mansoori, B.; Locke, S.J. Study of 4-Quinolone Antibiotics in
602 Biological Samples by Short-Column Liquid Chromatography Coupled with Electrospray
603 Ionization Tandem Mass Spectrometry. *Anal Chem*. **1997,** 69, 4143-4155.
604 41. Terzic, S.; Senta, I.; Matosic, M.; Ahel, M. Identification of biotransformation products
605 of macrolide and fluoroquinolone antimicrobials in membrane bioreactor treatment by
606 ultrahigh-performance liquid chromatography/quadrupole time-of-flight mass
607 spectrometry.) *Anal Bioanal Chem*. **2011,** 401, 353-363.
608 42. http://mzmine.sourceforge.net (17/01/2014)
609 43. Pluskal, T.; Castillo, S.; Villar-Briones, A.; Oresic, M. MZmine 2: Modular framework
610 for processing, visualizing, and analyzing mass spectrometry-based molecular profile data.
611 *Bioinformatics* **2010,** 11, 395-405
612 44. Wu, L.; Liu, D.Q. Data-dependent tandem mass spectrometry of doubly protonated
613 molecules in pharmaceutical analysis. *Rapid Commun Mass Spectrom*. **2007,** 21, 455-458.
614 45. Clemente, M.; Hermo, M.P.; Barrón, D.; Barbosa, J. Confirmatory and quantitative
615 analysis using experimental design for the extraction and liquid chromatography–UV,
616 liquid chromatography–mass spectrometry and liquid chromatography–mass
617 spectrometry/mass spectrometry determination of quinolones in turkey muscle. *J*
618 *Chromatogr A* **2006,** 1135, 170-178
619 46. Picó, Y.; Andreu, V. Fluoroquinolones in soil—risks and challenges. *Anal Bioanal*
620 *Chem*. **2007,** 387, 1287-1299.
621 47. Hermo, M.P.; Barrón, D.; Barbosa, J. Multiresidue determination of quinolones
622 regulated by the European Union in bovine and porcine plasma. Application of

chromatographic and capillary electrophoretic methodologies. *J Chromatogr A* **2008,** 1201, 1-14.

48. Kaufmann, A.; Butcher, P.; Maden, K.; Widmer, M.; Giles, K.; Uría, D. Are liquid chromatography/electrospray tandem quadrupole fragmentation ratios unequivocal confirmation criteria? *Rapid Commun Mass Spectrom*. **2009,** 23, 985-998.

49. Thermo Scientific Analytical Tools for Metabolism. Biotransformation Reference Guide 2009

50. http://foodbs.org/examples/milk. (17/01/2014)

51. Rust, H.; Scheer, M.; Hallenbach, W. BAYER AG, Preparation of quinolone and naphthylidinone N-oxides as antibacterials. Patent ES 2 161 361 T3.

52. Badertscher, M.; Bischofberger, K.; Munk, M.E.; Pretsch, E. A Novel Formalism to Characterize the Degree of Unsaturation of Organic Molecules. J Chem Inf Comput Sci. **2001,** 41, 889-893.

FIGURE CAPTIONS

Fig 1

Structures of the four quinolones studied (ENR, CIP, DIF and SAR).

Fig 2

A) MS^2 spectrum for the hydroxylated TP of DIF. B) MS^2 spectrum for the N-oxide TP of DIF.

Fig 3

A) EIC of ion *m/z* 390.1460 in the milk sample spiked with ENR. B) MS^2 spectrum for ENR. C) MS^2 spectrum for the first peak (t_R 5.71 min). D) MS^2 spectrum for the remaining peaks (t_R 7.57 and 7.99 min).

Fig 4

Product ion scan (MS^2) of CIP lactose conjugate (precursor ion *m/z* 656.2457). Top left, extended mass spectrum where losses of water molecules are shown.

Fig 5

Influence of the different warming conditions in areas of different TPs of ENR, CIP, DIF and SAR.

Fig 6

MS^2 spectra for the metabolites of ENR. A) *m/z* 263.0828 (ENR-1). B) *m/z* 291.0776 (ENR-2). C) *m/z* 307.1089 (ENR-4). D) *m/z* 348.1354 (ENR-9).

664 **TABLE OF CONTENTS GRAPHIC**

665

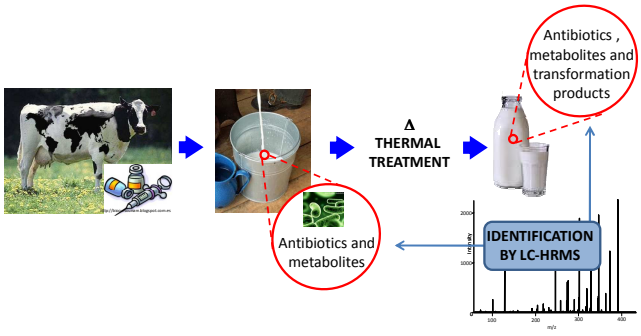

666

Table 1. Accurate masses of ions observed in milk spiked samples but not in blank milk samples by LC-ToF. The errors (ppm) are calculated from the theoretical and proposed structures.

ENR				**CIP**			
***m/z* (exp)**	***m/z* (theorical)**	**Structure**	**Error (ppm)**	***m/z* (exp)**	***m/z* (theorical)**	**Structure**	**Error (ppm)**
157.5685	157.5686	$[CIP+2H-H_2O]^{2+}$	0.6	**157.5690**	157.5686	$[CIP+2H-H_2O]^{2+}$	2.5
166.5740	166.5739	$[CIP+2H]^{2+}$	0.6	**166.5742**	166.5739	$[CIP+2H]^{2+}$	1.8
167.5820	n.a *	$[334.1569]^{2+}$	-	**274.0989**	n.a	n.a	-
171.5845	171.5843	$[ENR+2H-H_2O]^{2+}$	1.2	**288.1511**	288.1507	$[CIP+H-CO_2]^{+}$	1.4
180.5897	180.5897	$[ENR+2H]^{2+}$	0.1	**314.1293**	314.1288	$[CIP+H-H_2O]^{+}$	1.6
316.1817	316.1820	$[ENR+H-CO_2]^{+}$	0.9	**332.1400**	332.1405	$[CIP+H]^{+}$	1.5
332.1402	332.1405	$[CIP+H]^{+}$	0.9	**348.1334**	n.a	n.a	-
334.1569	n.a	n.a	-	**362.1148** [b]	n.a	n.a	-
342.1603	342.1612	$[ENR+H-H_2O]^{+}$	2.6	**374.1509**	n.a	n.a	-
360.1719	360.1718	$[ENR+H]^{+}$	0.3	**375.1563**	n.a	n.a	-
376.1656 [a]	n.a	n.a	-	**573.1431**	n.a	n.a	-
390.1461 [b]	n.a	n.a	-	**656.2477**	n.a	n.a	-
719.3349	719.3363	$[2ENR+H]^{+}$	1.9				
DIF				**SAR**			
***m/z* (exp)**	***m/z* (theorical)**	**Structure**	**Error (ppm)**	***m/z* (exp)**	***m/z* (theorical)**	**Structure**	**Error (ppm)**
191.5714	191.5717	$[DIF+2H-H_2O]^{2+}$	0.5	**184,5637**	184.5639	$[SAR+2H-H_2O]^{2+}$	1.1
200.5761	200.5770	$[DIF+2H]^{2+}$	3.0	**193,5692**	193.5692	$[SAR+2H]^{2+}$	0.1
299.0980	n.a	n.a	-	**342,1422**	342.1412	$[SAR+H-CO_2]^{+}$	2.9
374.1284	n.a	n.a	-	**360,1181**	n.a	n.a	-
382.1367	382.1362	$[DIF+H-H_2O]^{+}$	1.3	**368,1193**	368.1205	$[SAR+H-H_2O]^{+}$	3.3
386.2209	386.1311	$[SAR+H]^{+}$	0.3	**386.1311**	386.1311	$[SAR+H]^{+}$	0.1
400.1446	400.1467	$[DIF+H]^{+}$	2.0	**402.1241**	n.a	n.a	-
416.1396 [a]	n.a	n.a	-	**416,1069**	n.a	n.a	-
430.1185 [b]	n.a	n.a	-	**428.1410**	n.a	n.a	-
				429.1395	n.a	n.a	-

(*) n.a: Non-assigned.
(a) 2 chromatographic peaks with the same *m/z* (at different retention time).
(b) 3 chromatographic peaks with the same *m/z* (at different retention time).

Table 2. Accurate masses of parent quinolones, given reactions, all TPs observed and the fragments obtained by LC-LTQ-Orbitrap. The DBE calculated with the deprotonated molecular formula and the calculated error (ppm) of the assignation of structure.

	t_R [a] (min)	*m/z*	Gains or losses	Reactions (*)	*m/z* TPs	Fragmentation	Molecular formula	DBE	Theorical mass	Error (ppm)
Common reactions of 4 quinolones										
ENR	4.7	360.1718	+15.9949	HX	376.1666	358.1560, 340.1121, 286.1018, 244.0912, 243.0877	$C_{19}H_{23}FN_3O_4$	10	376.1667	-0.3
ENR	5.8	360.1718	+15.9949	N-O	376.1665	359.1639, 330,1611, 315.1741, 300.1506, 257.1085, 231.0928, 84.0807	$C_{19}H_{23}FN_3O_4$	10	376.1667	-0.5
CIP	3.6	332.1405	+15.9949	HX	348.1355	330.1248, 310.1184, 136.0617	$C_{17}H_{19}FN_3O_4$	10	348.1354	0.3
DIF	6.0	400.1467	+15.9949	HX	416.1416	398.1307, 343.0880, 329.0725, 316.0647, 256.0801	$C_{21}H_{20}F_2N_3O_4$	13	416.1416	0.0
DIF	6.3	400.1467	+15.9949	N-O	416.1418	399.1388, 370.1359, 355.1489, 299.09899	$C_{21}H_{20}F_2N_3O_4$	13	416.1416	0.5
SAR	5.8	386.1311	+15.9949	HX	402.1261	384.1156, 382.1197, 364.1089, 343.0882, 316.0653, 136.0758	$C_{20}H_{18}F_2N_3O_4$	13	402.1260	0.2
ENR	5.8	360.1718	+ 29.9740	HX + K	390.1458	372.1353, 362.1509, 346.1560, 318.1246, 301.0982, 289.09813, 245.1083, 128.0706, 100.0756, 72.0808	$C_{19}H_{21}FN_3O_5$	11	390.1460	-0.5
ENR	6.7	360.1718	+ 29.9740	HX + K	390.1462	372.1356, 362.1510, 291.07754, 273.0670, 259.0514, 100.0757, 72.0808	$C_{19}H_{21}FN_3O_5$	11	390.1460	0.5
ENR	6.8	360.1718	+ 29.9740	HX + K	390.1461	372.1355, 362.1509, 291.0774, 273.0669, 259.0513, 100.0756, 72.0809	$C_{19}H_{21}FN_3O_5$	11	390.1460	0.3
CIP	6.1	332.1405	+ 29.9740	HX + K	362.1141[b]		$C_{17}H_{17}FN_3O_5$	11	362.1147	-1.7
DIF	6.0	400.1467	+ 29.9740	HX + K	430.1209	412.1102, 402.1259, 386.1309, 368.1204, 329,0730, 299.0988, 197.1029, 114.0549, 70.0650	$C_{21}H_{18}F_2N_3O_5$	14	430.1209	0.0
DIF	6.9	400.1467	+ 29.9740	HX + K	430.1207	412.1101, 402.1258, 384.1151, 345.0678, 327.0572, 86.0599	$C_{21}H_{18}F_2N_3O_5$	14	430.1209	-0.5
DIF	7.1	400.1467	+ 29.9740	HX + K	430.1207	412.1101, 402.1258, 384.1151, 345.0678, 327.0572, 86.0599	$C_{21}H_{18}F_2N_3O_5$	14	430.1209	-0.5
SAR	6.7	386.1311	+ 29.9740	HX + K	416.1053[b]		$C_{20}H_{16}F_2N_3O_5$	14	416.1053	0.0
ENR	4.4	360.1718	- 26.0146	DE + H	334.1560	316.1464, 311.3906, 296.1393, 289.098, 263.0825, 219.0927, 164.1069, 86.0600, 72.0807	$C_{17}H_{21}FN_3O_3$	9	334.1561	-0.3
CIP	3.6	332.1405	- 26.0146	DE + H	306.1246	288.1141, 268.108, 263.0824, 245.1084	$C_{15}H_{17}FN_3O_3$	9	306.1248	-0.7
DIF	5.8	400.1467	- 26.0146	DE + H	374.1307	354.1246, 343.0884, 336.1138, 317.0728, 299.0988, 280.1242, 273.0830	$C_{19}H_{18}F_2N_3O_3$	12	374.1311	-1.1
SAR	5.9	386.1311	- 26.0146	DE + H	360.1156	343.0883, 342.1048, 340.1089, 322.0986, 317.07310, 299.0991	$C_{18}H_{16}F_2N_3O_3$	12	360.1154	0.6

Other reactions										
ENR	5.0	360.1718	- 28.0303	DE	332.1404		$C_{17}H_{19}FN_3O_3$	10	332.1405	-0.3
DIF	6.0	400.1467	- 14.0157	DM	386.1309		$C_{20}H_{18}F_2N_3O_3$	13	386.1311	-0.5
CIP	7.0	332.1405	+ 42.0103	A	374.1509	356.1402, 314.1297, 300.0777, 272.0827, 249.0669, 243.0563, 231.0562, 215.0249	$C_{19}H_{21}FN_3O_4$	11	374.1511	-0.5
SAR	8.0	386.1311	+ 42.0103	A	428.1416	410.1310, 382.1361, 368.1203	$C_{22}H_{20}F_2N_3O_4$	14	428,1416	0.0
CIP	6.6	332.1405	+ 43.0056	F	375.1463	357.1356, 340.1096, 332.1402, 314.1297, 270.0671, 243.0563, 231.0563, 216.0692	$C_{18}H_{20}FN_4O_4$	11	375.1463	0.0
SAR	7.2	386.1311	+ 43.0056	F	429.1369	411.1264, 386.1312, 368.1205, 348.1141	$C_{21}H_{19}F_2N_4O_4$	14	429.1369	0.0
CIP	5.0	332.1405	- 58.0419	DY +DCP	274.0986[c]	231.0562[c], 217.0404[c], 203.0611, 187.0663, 175.0664, 163.0665, 148.0556, 136.557 [c]	$C_{14}H_{13}FN_3O_2$	10	274.0986	0.0
CIP	5.0	332.1405	+ 241.0024		573.1429[b]					
CIP	4.0	332.1405	+ 324.1056	LC	656.2457	638.2450, 620.2246, 494.1929, 476.1825, 404.1616, 344.1400, 332.1401	$C_{29}H_{39}FN_3O_{13}$	12	656.2461	-0.6

[a] Retention time when LC-ToF is used.

[b] Concentration too low to be fragmented; [c] These masses were also observed with a molecule of water (+ 18.0105) but at low concentration.

(*) HX: hydroxylation; N-O: N-Oxide; K: ketone formation; DE: deethylation; H: Hydrogenation; CC: cysteine conjugation; DC: Decarboxylation; DF: Reductive defluorination; DM: Demethylation; A: Acetylation; F: Formamidation; DY: Dehydration; DCP: Decyclopropylation; LC: Lactose conjugation.

Table 3. Metabolites and TPs found in medicated cow milk with ENR sorted by accurate mass. Accurate masses analysed by ToF and Orbitrap and their theorical mass assigned to molecular formula are given with calculated error (ppm) for the assignation of suggested structure for the two analysers.

***m/z* (ToF)**	***m/z* (Orbitrap)**	***m/z* theorical**	**t_R [a] (min)**	**Molecular formula [b]**	**Error (ppm) (ToF)**	**Error (ppm) (Orbitrap)**	**Suggested Structure**	**DBE**	
263.0828	263.0834	263.0826	6.85	$C_{13}H_{12}FN_2O_3^+$	0.8	3.0	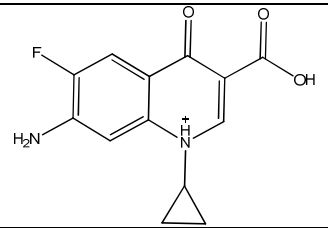	9	ENR-1
288.1349	288.1345	288.1343	2.9	$C_{15}H_{18}O_3N_3^+$	2.1	0.7	n.a		
291.0770	291.0783	291.0776	6.7	$C_{14}H_{12}FN_2O_4^+$	-2.1	2.4	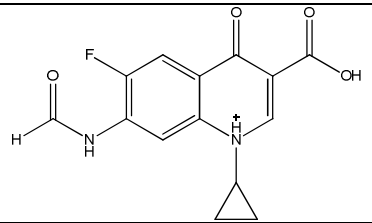	10	ENR-2
302.1501	302.1506	302.1499	5.7	$C_{16}H_{20}N_3O_3^+$	0.7	2.3	n.a		
306.1239	306.1256	306.1248	3.6	$C_{15}H_{17F}N_3O_3^+$	-2.9	2.6	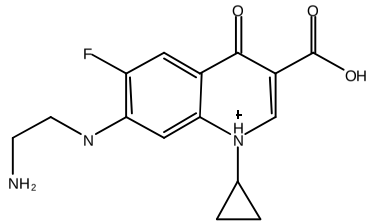	9	ENR-3
307.1083	307.1097	307.1089	6.5	$C_{15}H_{16}FN_2O_4^+$	-1.9	1.9	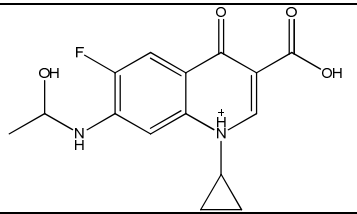	9	ENR-4
329.1485	329.1498	329.1496	3.4	$C_{18}H_{21}N_2O_4^+$	-3.3	0.6	n.a		
329.1485	329.1498	329.1496	4.9	$C_{18}H_{21}N_2O_4^+$	-3.3	0.6	n.a		

332.1408	332.1405	332.1405	5.0	$C_{17}H_{19}FN_3O_3^+$	0.9	0	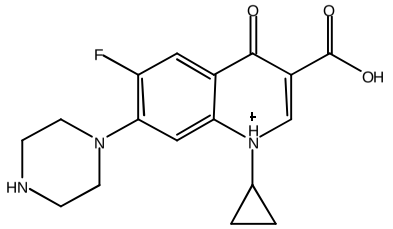	10	CIP
334.1189	334.1207	334.1198	6.4	$C_{16}H_{17}FN_3O_4^+$	-2.7	2.7	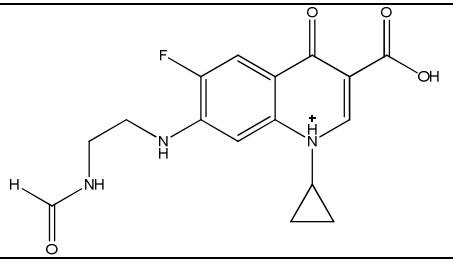	10	ENR-5
334.1539	334.1566	334.1561	4.35	$C_{17}H_{21}FN_3O_3^+$	-6.5	1.5	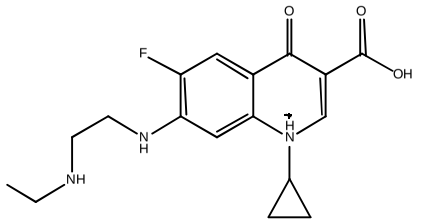	9	ENR-6
346.1190	346.1204	346.1198	6.5	$C_{17}H_{17}FN_3O_4^+$	-2.3	1.7	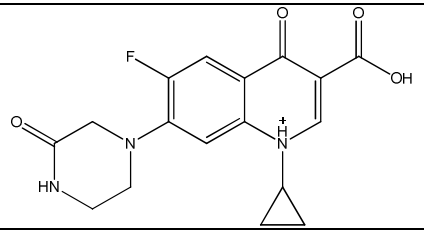	11	ENR-7
348.1343	348.1350	348.1354	3.6	$C_{17}H_{19}FN_3O_4^+$	-3.1	-1.1	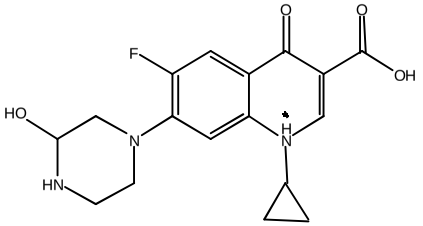	10	ENR-8

348.1343	348.1364	348.1354	6.5	$C_{17}H_{19}FN_3O_4^+$	-3.1	2.9	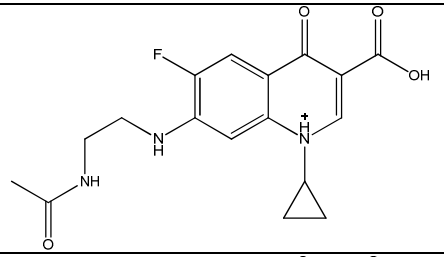	10	ENR-9
360.1357	360.1360	360.1354	6.9	$C_{18}H_{19}FN_3O_4^+$	0.8	1.7	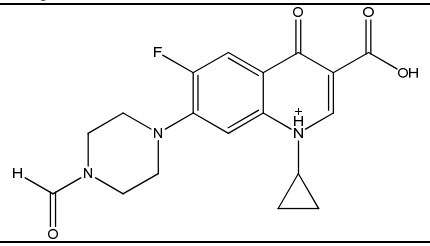	11	ENR-10
362.1137	362.1152	362.1147	6.1	$C_{17}H_{17}FN_3O_5^+$	-2.8	1.4	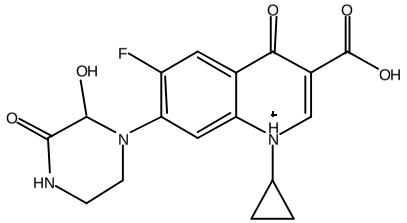	11	ENR-11
362.1137	362.1152	362.1147	6.8	$C_{17}H_{17}FN_3O_5^+$	-2.8	1.4	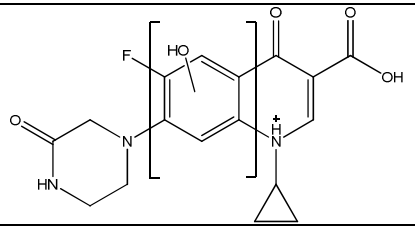	11	ENR-12
362.1137	362.1152	362.1147	7.1	$C_{17}H_{17}FN_3O_5^+$	-2.8	1.4		11	ENR-13
374.1510	374.1523	374.1511	7.0	$C_{19}H_{21}FN_3O_4^+$	-0.3	2.7	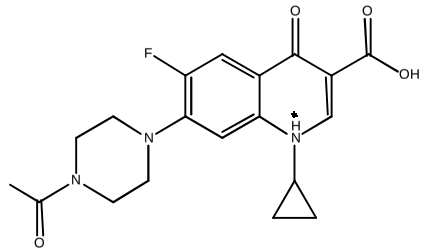	11	ENR-14

375.1462	375.1464	375.1463	6.6	$C_{18}H_{20}FN_4O_4^+$	-0.3	0.3	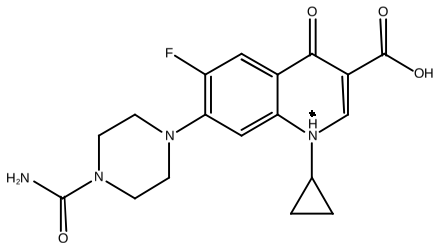	11	ENR-15
376.1656	376.1671	376.1667	4.6	$C_{19}H_{23}FN_3O_3^+$	-2.9	1.1	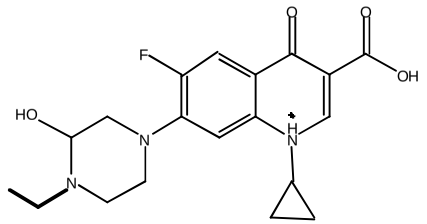	10	ENR-16
376.1656	376.1673	376.1667	5.8	$C_{19}H_{23}FN_3O_3^+$	-2.9	1.6	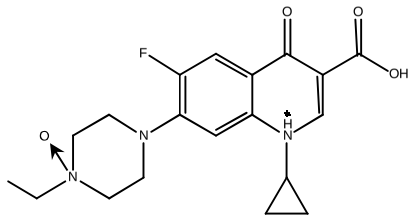	10	ENR-17
390.1459	390.1461	390.1460	6.65	$C_{19}H_{21}FN_3O_5^+$	-0.3	0.3	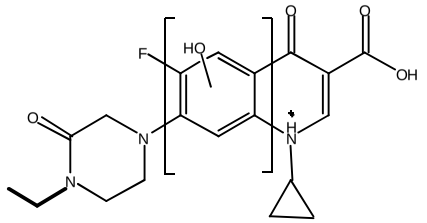	11	ENR-18
390.1459	390.1461	390.1460	6.85	$C_{19}H_{21}FN_3O_5^+$	-0.3	0.3		11	ENR-19

[a] Retention time when LC-ToF is used.
[b] These molecular formulas are hypothetical in case of metabolites without assigned structure.
n.a : Non-assigned

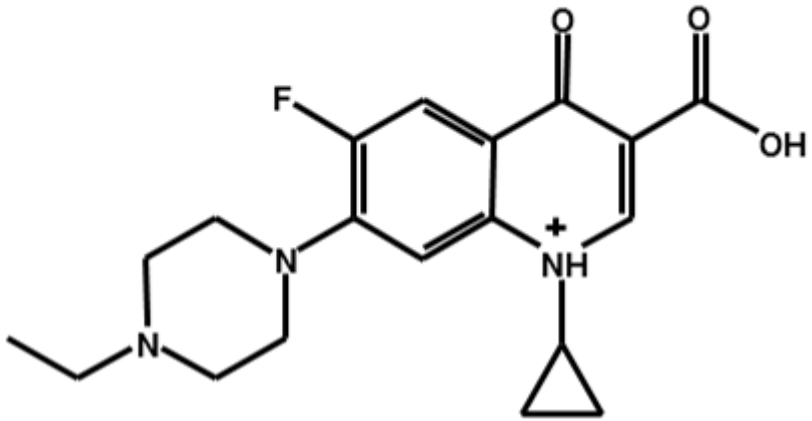

ENR
m/z 360.1718

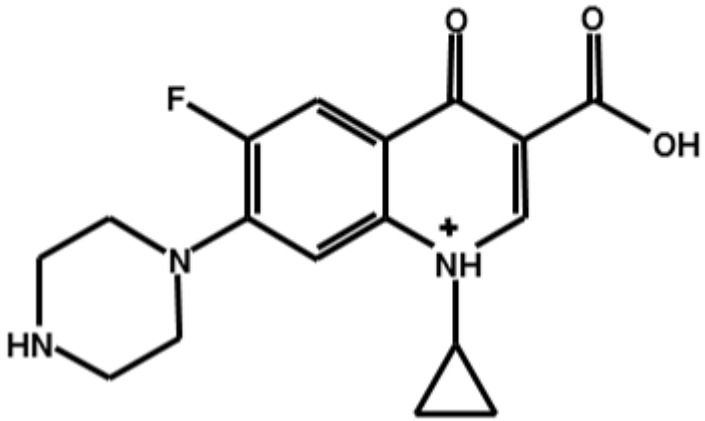

CIP
m/z 332.1405

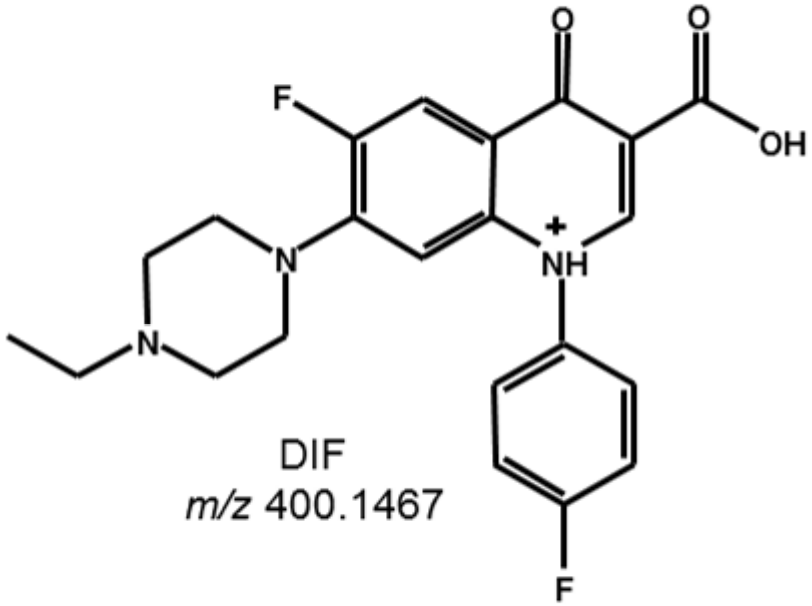

DIF
m/z 400.1467

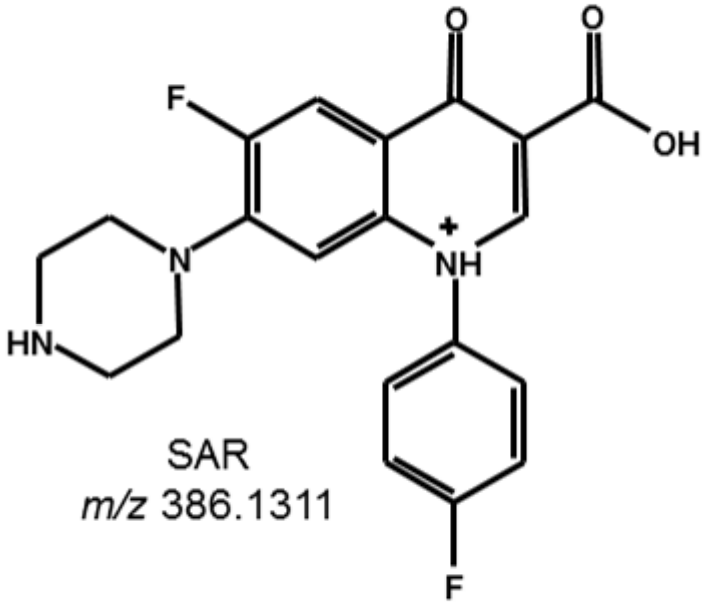

SAR
m/z 386.1311

Fig 1

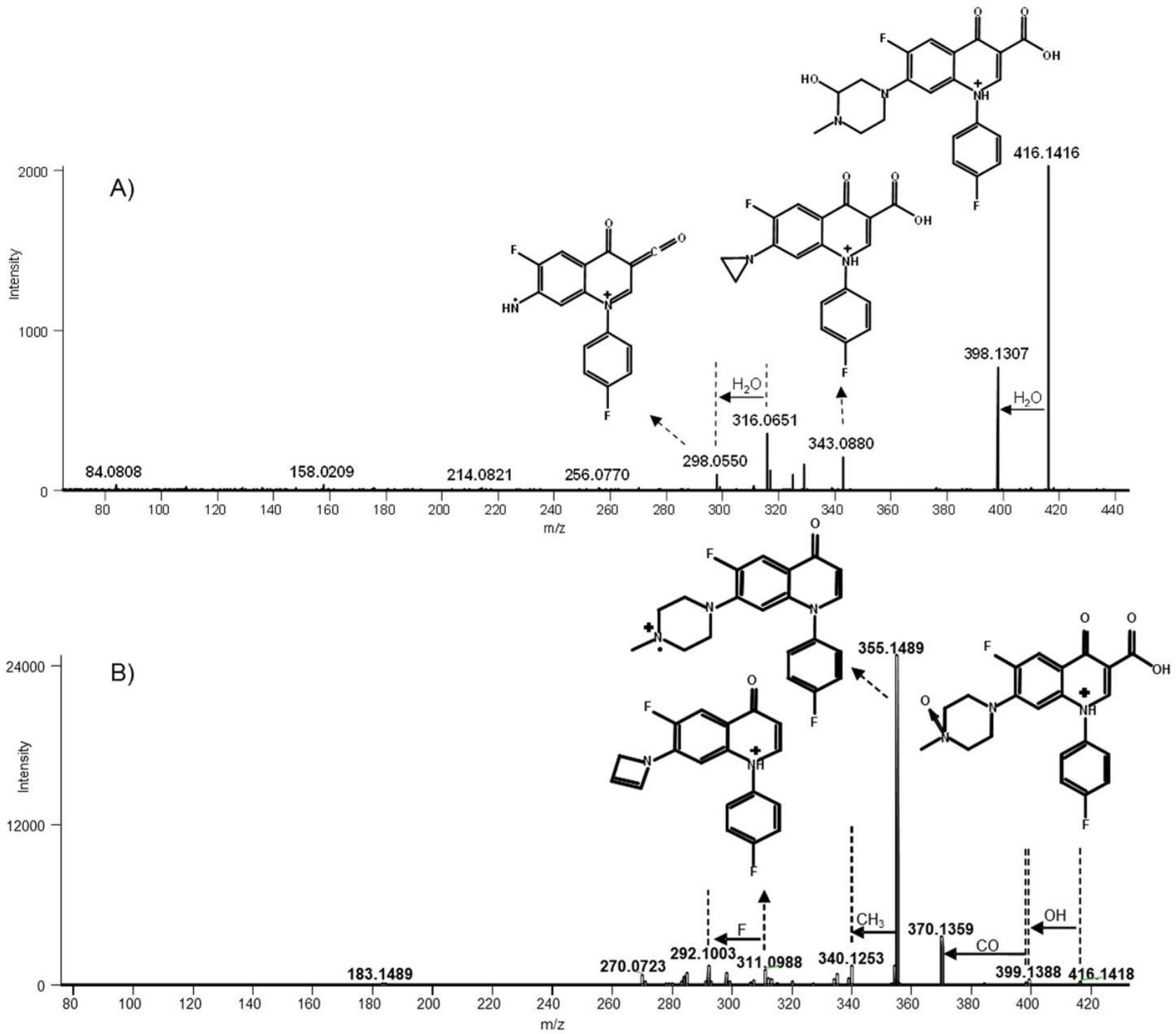
A)
Intensity
2000
1000
0
84.0808
158.0209
214.0821
256.0770
298.0550
316.0651
343.0880
398.1307
416.1416
H_2O
H_2O
80 100 120 140 160 180 200 220 240 260 280 300 320 340 360 380 400 420 440
m/z
B)
Intensity
24000
12000
0
183.1489
270.0723
292.1003
311.0988
340.1253
355.1489
370.1359
399.1388
416.1418
F
CH_3
CO
OH
80 100 120 140 160 180 200 220 240 260 280 300 320 340 360 380 400 420
m/z

Fig 2

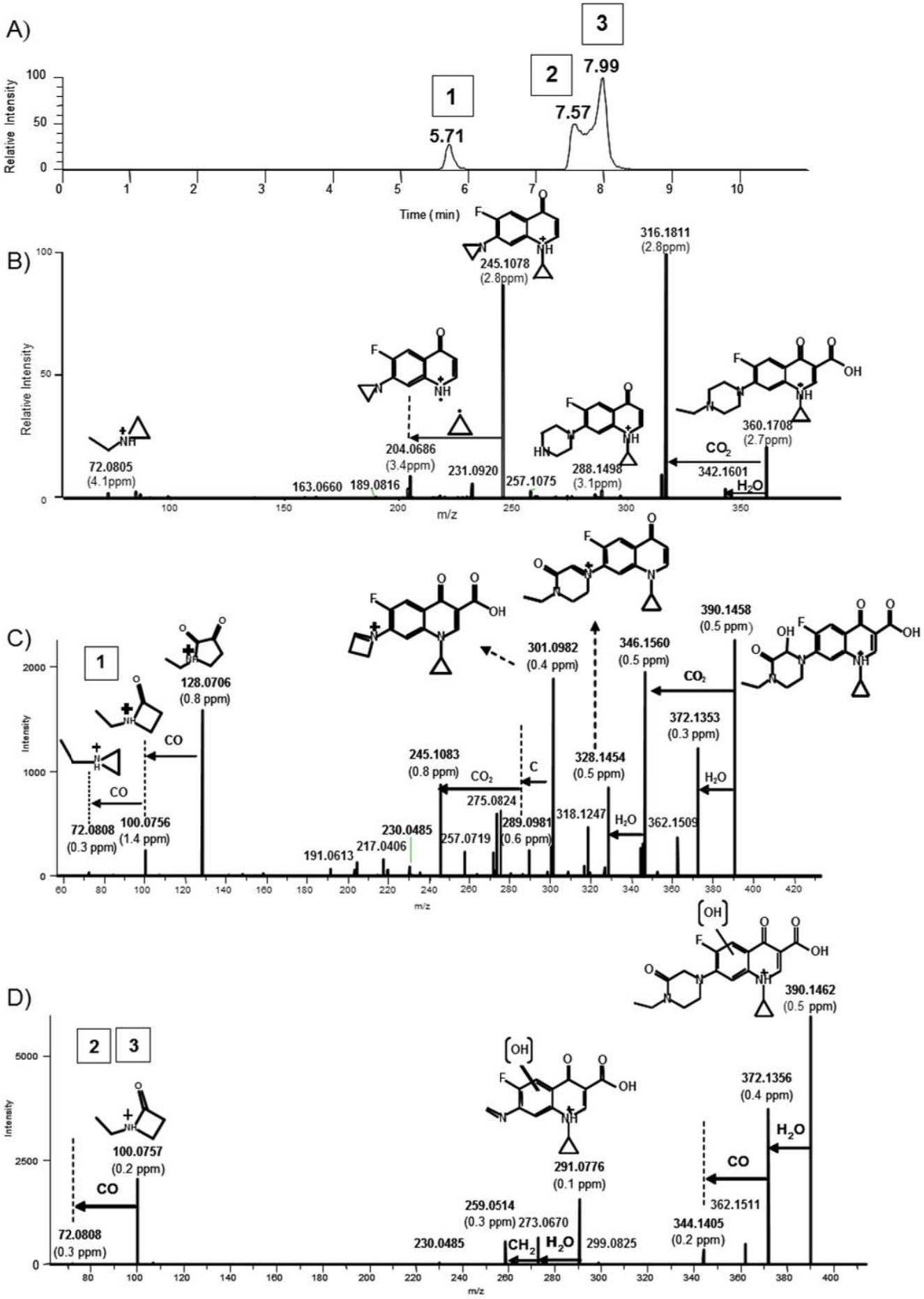
A)
1
2
3
5.71
7.57
7.99
Relative Intensity
Time (min)
B)
245.1078
(2.8ppm)
316.1811
(2.8ppm)
204.0686
(3.4ppm)
360.1708
(2.7ppm)
72.0805
(4.1ppm)
163.0660
189.0816
231.0920
257.1075
288.1498
(3.1ppm)
342.1601
CO2
H2O
m/z
C)
1
128.0706
(0.8 ppm)
CO
CO
72.0808
(0.3 ppm)
100.0756
(1.4 ppm)
245.1083
(0.8 ppm)
CO2
C
301.0982
(0.4 ppm)
328.1454
(0.5 ppm)
346.1560
(0.5 ppm)
390.1458
(0.5 ppm)
372.1353
(0.3 ppm)
H2O
275.0824
289.0981
(0.6 ppm)
318.1247
H2O
362.1509
230.0485
217.0406
257.0719
191.0613
Intensity
m/z
D)
2
3
100.0757
(0.2 ppm)
CO
72.0808
(0.3 ppm)
291.0776
(0.1 ppm)
259.0514
(0.3 ppm)
273.0670
230.0485
CH2
H2O
299.0825
344.1405
(0.2 ppm)
362.1511
CO
372.1356
(0.4 ppm)
H2O
390.1462
(0.5 ppm)
Intensity
m/z

Fig 3

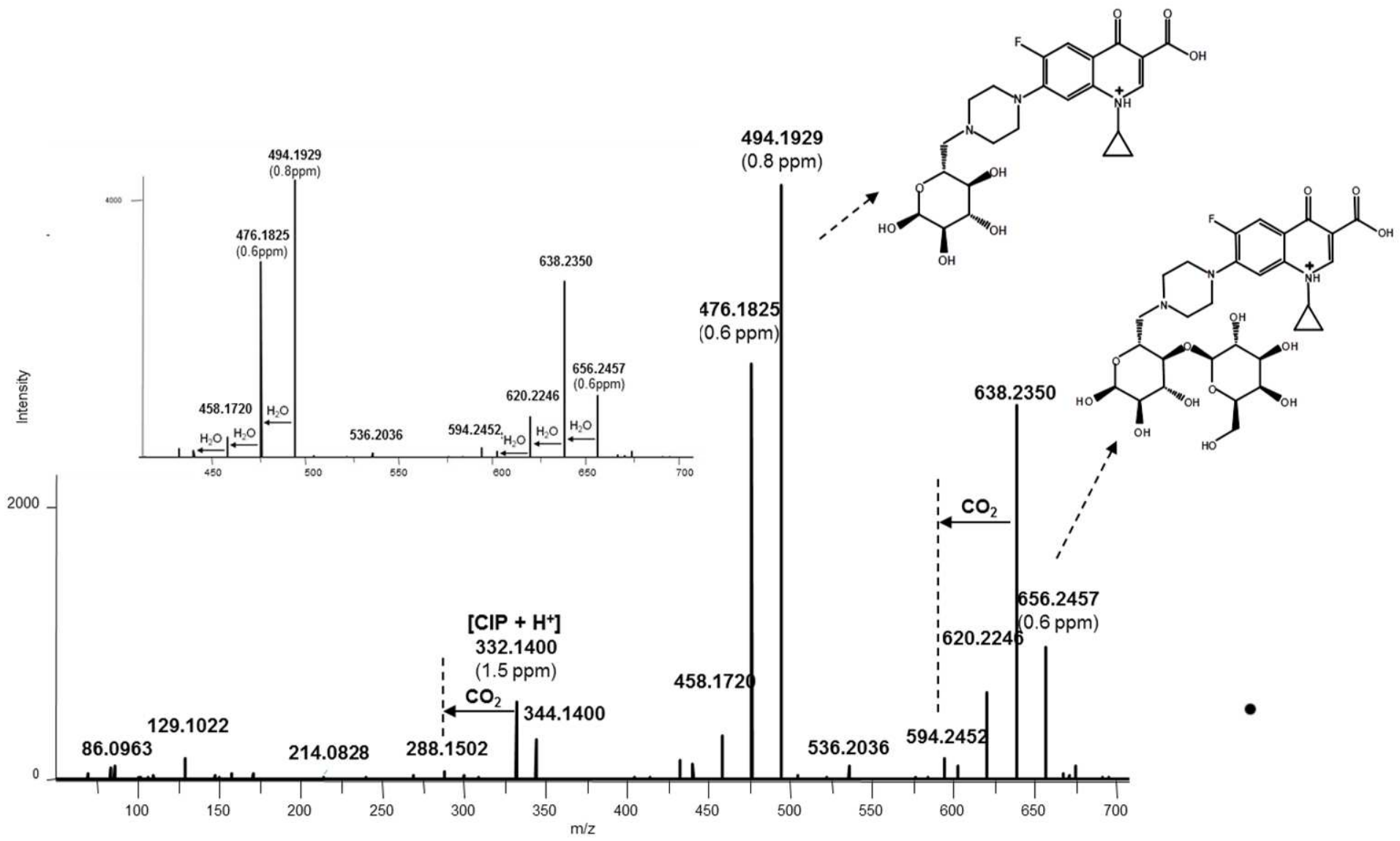
494.1929
(0.8ppm)
476.1825
(0.6ppm)
638.2350
656.2457
(0.6ppm)
620.2246
458.1720
536.2036
594.2452
494.1929
(0.8 ppm)
476.1825
(0.6 ppm)
638.2350
656.2457
(0.6 ppm)
620.2246
[CIP + H+]
332.1400
(1.5 ppm)
CO2
344.1400
458.1720
129.1022
86.0963
214.0828
288.1502
536.2036
594.2452
Intensity
m/z

Fig 4

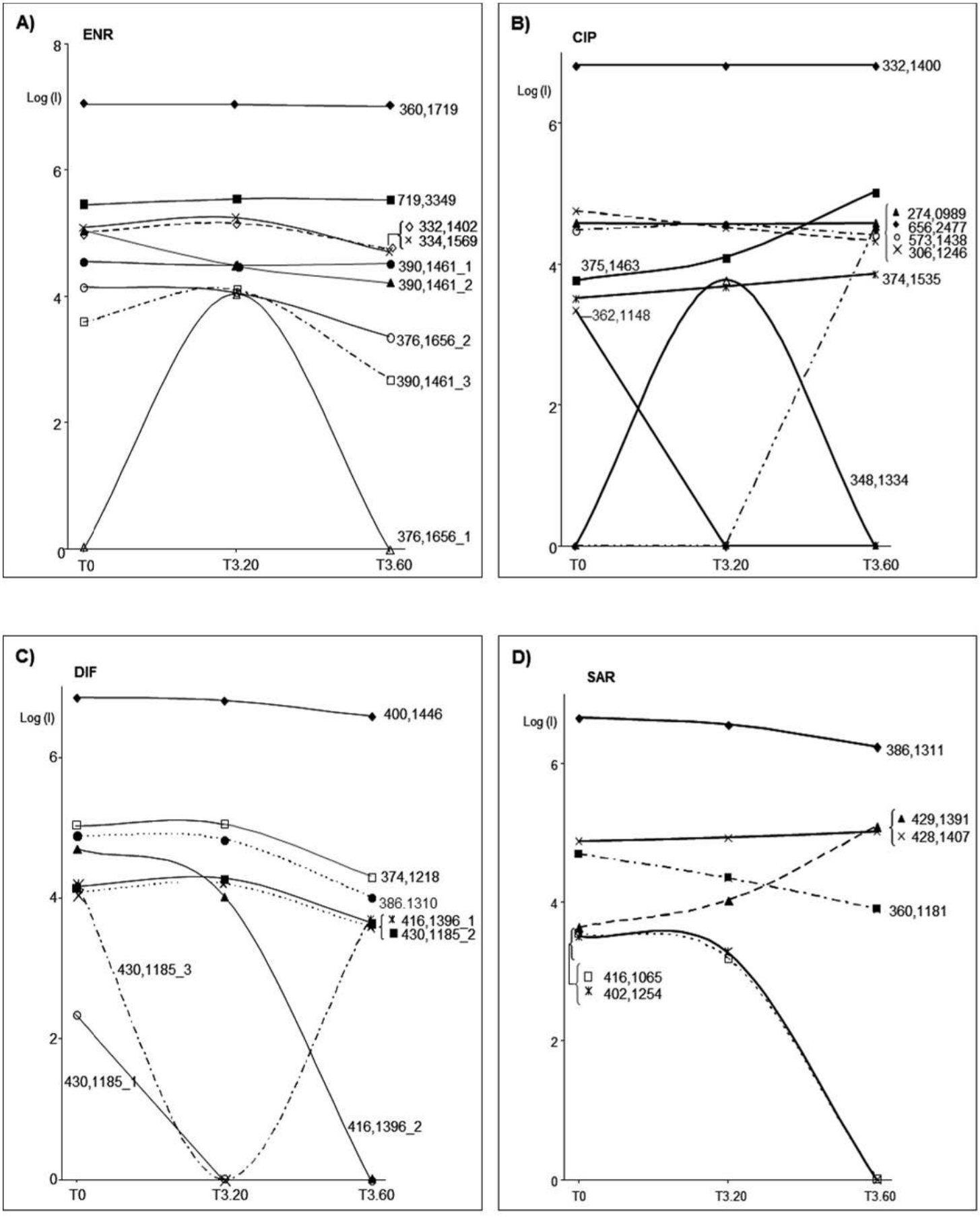
A)
ENR
Log (l)
8
6
4
2
0
360,1719
719,3349
332,1402
334,1569
390,1461_1
390,1461_2
376,1656_2
390,1461_3
376,1656_1
T0
T3.20
T3.60
B)
CIP
Log (l)
6
4
2
0
332,1400
274,0989
656,2477
573,1438
306,1246
375,1463
374,1535
362,1148
348,1334
T0
T3.20
T3.60
C)
DIF
Log (l)
6
4
2
0
400,1446
374,1218
386.1310
416,1396_1
430,1185_2
430,1185_3
430,1185_1
416,1396_2
T0
T3.20
T3.60
D)
SAR
Log (l)
6
4
2
0
386,1311
429,1391
428,1407
360,1181
416,1065
402,1254
T0
T3.20
T3.60

Fig 5

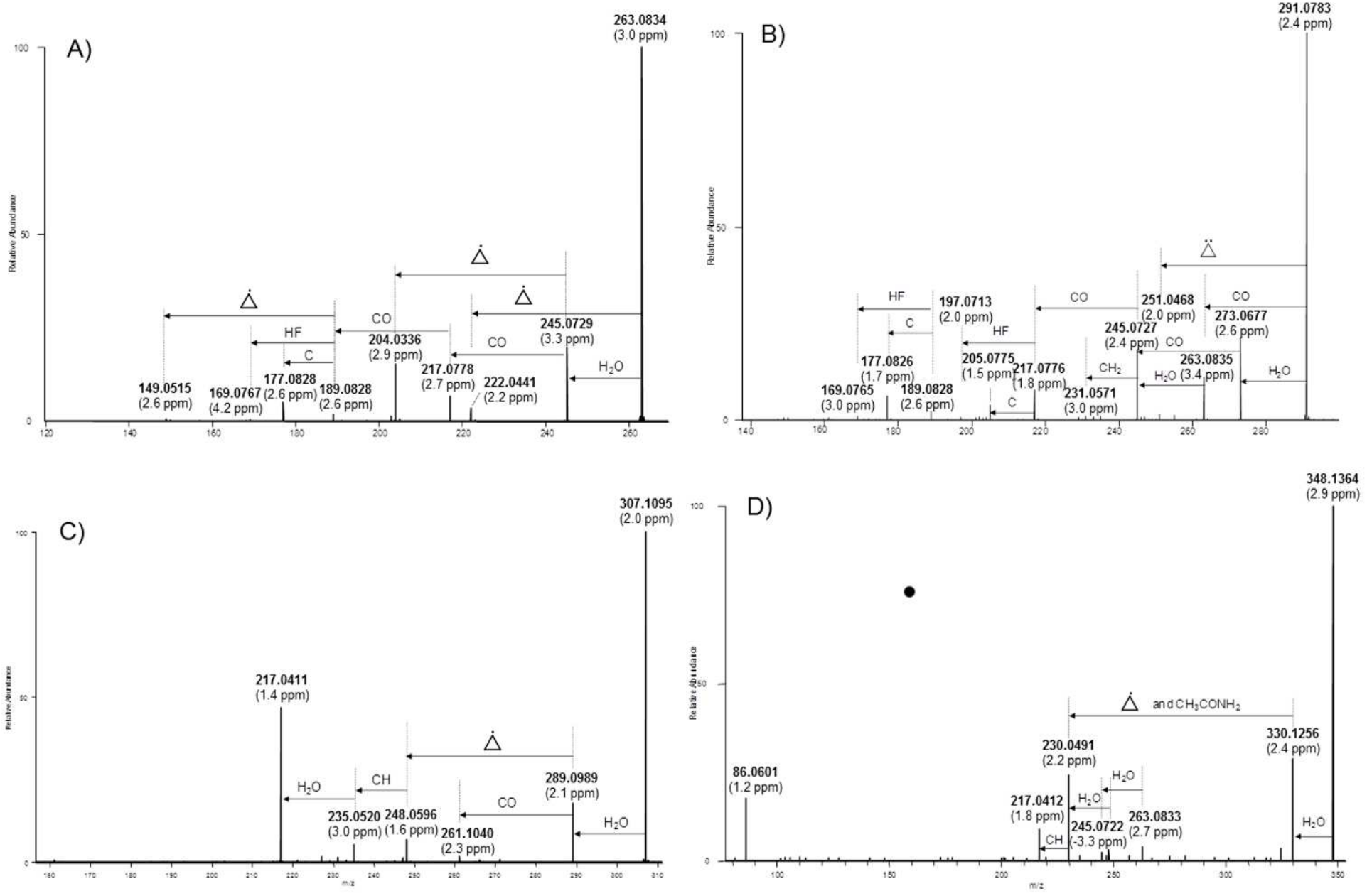
A)
263.0834
(3.0 ppm)
HF
CO
C
204.0336
(2.9 ppm)
CO
245.0729
(3.3 ppm)
H2O
149.0515
(2.6 ppm)
169.0767
(4.2 ppm)
177.0828
(2.6 ppm)
189.0828
(2.6 ppm)
217.0778
(2.7 ppm)
222.0441
(2.2 ppm)
B)
291.0783
(2.4 ppm)
HF
197.0713
(2.0 ppm)
C
CO
251.0468
(2.0 ppm)
CO
273.0677
(2.6 ppm)
245.0727
(2.4 ppm)
CO
HF
177.0826
(1.7 ppm)
205.0775
(1.5 ppm)
217.0776
(1.8 ppm)
CH2
263.0835
H2O (3.4 ppm)
H2O
169.0765
(3.0 ppm)
189.0828
(2.6 ppm)
C
231.0571
(3.0 ppm)
C)
307.1095
(2.0 ppm)
217.0411
(1.4 ppm)
H2O
CH
289.0989
(2.1 ppm)
CO
H2O
235.0520
(3.0 ppm)
248.0596
(1.6 ppm)
261.1040
(2.3 ppm)
D)
348.1364
(2.9 ppm)
and CH3CONH2
330.1256
(2.4 ppm)
230.0491
(2.2 ppm)
H2O
86.0601
(1.2 ppm)
H2O
217.0412
(1.8 ppm)
263.0833
(2.7 ppm)
245.0722
(-3.3 ppm)
CH
H2O

Fig 6

Electronic Supporting Information for the research article:

IDENTIFICATION OF METABOLITES AND THERMAL TRANSFORMATION PRODUCTS OF QUINOLONES IN RAW COW MILK BY LIQUID CHROMATOGRAPHY COUPLED TO HIGH RESOLUTION MASS SPECTROMETRY

A. Junza[1], S. Barbosa[2], R. Codony[3], A. Jubert[3], J. Barbosa[1,2], D. Barrón[1]*

[1]Departament de Química Analítica, Campus de l'Alimentació de Torribera

Avda. Prat de la Riba, 171, 08921 Sta. Coloma de Gramanet, Barcelona, Spain

[2]Departament de Química Analítica

Martí Franquès, 1-11, 08028 Barcelona, Spain

[3] Laboratori Interprofessional Lleter de Catalunya (ALLIC)

Ctra. Vilassar a Cabrils s/n, 08348 Cabrils, Barcelona,

* Email: dolores.barron@ub.edu

Content:

Section 3.2: Common reactions of the four quinolones

1. **TPs of DIF (*m/z* 416.1416)**

In the mass spectrum of the ion *m/z* 416.1416 (Figure 2A), two losses of water (18.0105 *m/z*) were observed. The first was due to carboxylic acid and the same loss was observed for the rest of the quinolones. The second loss of water observed in the spectra is only possible if an OH group is in position 2 or 3 of the piperazine ring.

2. **TPs of ENR (*m/z* 390.1460) Peak 1**

The accurate mass of the fragment *m/z* 128.0706 corresponds to molecular formula $C_6H_{10}NO_2$ with a DBE value of 3 and is the key to the elucidation (Figure 3C). This was followed by two consecutive fragmentations, corresponding to losses of 27.9949 (CO) [128.0706 - CO → 100.0756; 100.0756 - CO → 72.0808] and the reduction of one unit of DBE. These fragments indicate that a ketone and an alcohol are present in the piperazinyl ring, as observed in the suggested fragmentation shown in Figure 3C. The rest of the fragments are due to losses of CO_2, H_2O and pieces of the piperazine ring. It should be noted that the DBE of some fragments such as *m/z* 301.0982 and 328.1454 are 10.5. The structures represented in the mass spectrum (Figure 3C) have 11 unsaturations (double bonds and rings). The DBE calculated is the average of the resonance structures of drawn structure (DBE: 11) and the carbocation (DBE:10)[52].

Section 3.2: Other reactions

1. **TPs of CIP and SAR (acetylation and formamidation)**

Two different reactions took place on CIP and SAR. The first was acetylation, which could be justified by a loss of acetyl group (42.0103) (Acetyl-CIP(-H_2O): 356.1402 → 314.1297 and Acetyl-SAR(-H_2O): 410.1310 → 368.1203), as observed in the MS spectra (not shown). The second reaction corresponds to formamidation. For CIP and SAR, the loss of formamide and subsequent gain of 2H occurred in one step (Formamide-CIP(-H_2O): 357.1356 → 314.1296 and Formamide-SAR(-H_2O): 411.1264 → 368.1205). Moreover, in the case of CIP, the loss of NH_3 (357.1356 → 340.1096), followed by the loss of a carbonyl and gain of 2H (340.1096 → 314.1296), were also observed. Due to the absence of the alkyl chain in the N^4-piperazinyl ring, both reactions (acetylation and formamidation) took place.

2. **TPs of CIP (*m/z* 656.2457)**

Figure 4 shows the mass spectrum of this TP with its fragmentations. The two main characteristic losses were the loss of -180.0633 (656.2457 → 476.1825), which corresponds to the loss of a glucose, and the loss of a galactose without a water molecule (476.1825 → 344.1400). In the spectrum, steady losses of six water molecules were observed due to the OH present on the sugars, as can be seen in the smaller mass spectrum in Figure 4. All these losses could be explained if the molecule CIP (332.1405) is combined with the lactose (galactose + glucose) present in milk at high concentration. This new product was favoured when samples were heated at a high temperature for a long time (60 min).

Section 3.4: Determination of metabolites and TPs in medicated cow milk

1. **Metabolite ENR-1 (*m/z* 263.0834)**

In the MS/MS spectrum of ENR-1 (Figure 6A), the loss of a water molecule (263.0834 → 245.0729) and CO (245.0729 → 217.0778) from carboxylic acid can be observed. The presence of cyclopropyl can also be justified by ion *m/z* 222.0441, which is the result of the loss of cyclopropyl from the parent metabolite (263.0834 – 41.0391 → 222.0441).

2. **Metabolite ENR-4 (*m/z* 307.1095)**

In this case, characteristic losses of the carboxylic group and cyclopropyl could be observed in the spectrum of ENR-4 (Figure 6C). The modifications of structure with respect to ENR, were again found over the piperazine ring. As can be seen, the ion *m/z* 248.0596 loses the methyl group, which results in the ion *m/z* 235.0520 that later loses a molecule of water (235.0520 → 217.0411).